Acta Crystallographica Section A
Foundations of Crystallography
ISSN 0108-7673

Received 28 December 2002
Accepted 18 March 2003

Relations between the zinc-blende and the NaCl structure type

H. Sowa

Institut für Angewandte Geowissenschaften, Allgemeine und Angewandte Mineralogie, Technische Universität BH1, Ernst-Reuter-Platz 1, D-10587 Berlin, Germany. Correspondence e-mail: heidrun.sowa@t-online.de

A new model for the transformation from the zinc-blende to the NaCl type is developed on the basis of the deformation of a 4-connected heterogeneous sphere packing in space group $P3_2$. The geometrical features of this transition are discussed by investigating the analogous deformations of a 4-connected homogeneous sphere packing in the supergroup $P3_221$ of $P3_2$. In this space group, the atomic arrangement corresponds to a diamond configuration. During the phase transition, it is deformed under preservation of all sphere contacts until a cubic primitive lattice is reached, the analogue of the NaCl arrangement formed by like atoms. The intermediate structure that occurs between the zinc-blende and the NaCl type is compared with the cinnabar type.

1. Introduction

Understanding the mechanisms of phase transformations is a challenging problem in crystal chemistry. It is known that diffusionless phase transitions accompanied by atomic shifts and shears can often be described within a common sub- or supergroup of the space groups of both modifications involved (*cf. e.g.* Dmitriev *et al.*, 1988; Christy, 1993; O'Keeffe & Hyde, 1996; Zunger *et al.*, 2001). Even phase transitions usually termed 'reconstructive' may be regarded in an analogous way if the intermediate structure can be obtained by a step-by-step symmetry reduction leading to a sequence of subgroups of the space groups of both phases. Christy (1993) pointed out that the shortest transformation pathway may be found by considering shared structural features of the two phases and the lattice modes that preserve these features while changing the rest of the structure. More complicated routes that may be energetically favoured can be obtained by interpolating additional steps. Christy (1993) gives some examples to illustrate such a process.

Besides such an intuitive search for common structural characteristics, a further method for the derivation of possible transition paths has been described (Sowa, 2000*a*,*b*, 2001). A transition mechanism can be modelled if a common subgroup of the space groups of the phases before and after the phase transformation is found that allows a deformation of one structure type into the other. Such a consideration is closely related to the analysis of corresponding lattice modes, but shared structural features must not be known. In some recent papers, this method has successfully been applied to transformations occurring in simple compounds. Transition mechanisms have been proposed for the pressure-induced transformations from the zinc-blende (Sowa, 2000*b*) and from the wurtzite type (Sowa, 2001) to the NaCl type. Phase transitions in elements and *AB* compounds were described by means of sphere-packing deformations: In these structures, all atoms together form a sphere packing. The phase that contains the lower coordinated atoms is regarded as the starting phase and it is assumed that no bonds are broken during the transition into the final phase.

The transition from the zinc-blende to the NaCl type is a good example for showing how difficult it is to find unchanged structural features common in the starting and in the final phase even in such simple compounds: zinc-blende crystallizes in the space group $F\bar{4}3m$. The atoms are located at the positions 4(*a*) 0,0,0 and 4(*c*) $\frac{1}{4},\frac{1}{4},\frac{1}{4}$. After the pressure-induced phase transition at about 15 GPa, an NaCl-type modification of ZnS becomes stable (*e.g.* Ves *et al.*, 1990). Analogous phase transformations have been observed in many compounds.

In crystal structures of both types, the cations as well as the anions form cubic face-centred lattices that are shifted against each other by a vector $(\frac{1}{4},\frac{1}{4},\frac{1}{4})$ in the case of the zinc-blende type and by a vector $(\frac{1}{2},\frac{1}{2},\frac{1}{2})$ in the case of the NaCl type. For obvious reasons, a transition mechanism may be suggested that implies a movement of the entire cation substructure against the anion substructure along one of the ⟨111⟩ directions. Then, the intermediate phase would have the symmetry $R3m$. However, the consequence of such a mechanism would be the breaking of one bond per atom. Therefore, the energy barrier for the corresponding atomic motions is too high, for instance, for GaAs and for boron compounds of the zinc-blende type (*cf.* Froyen & Cohen, 1983; Wentzcovitch *et al.*, 1987).

The mechanism proposed by Sowa (2000*b*) on the basis of symmetry reduction to $Imm2$ involves shifts of the cations and anions against each other along one of the ⟨001⟩ directions.

Adjacent atoms move in opposite directions and all nearest neighbours are maintained during the transition. In this case, the common feature of the two structures is the existence of four identical nearest neighbours, but this cannot be recognized by looking only at the starting and the final phases.

Independently, Shimojo *et al.* (2000) found a very similar transition path in performing molecular dynamics simulations of the pressure-induced phase transition in SiC. They described the intermediate phase as being monoclinic. However, Catti (2001) showed that it is orthorhombic and, using *ab initio* density-functional theory (DFT) methods, he proved that the activation energy for this mechanism is much lower than that with $R3m$ symmetry.

The present paper aims to find a further path for the zinc-blende to NaCl-type transition.

2. Symmetry relations between the zinc-blende and the NaCl type

The zinc-blende structure may be described as a heterogeneous sphere packing with four contacts per sphere while in the NaCl-type structure all atoms together form a heterogeneous sphere packing with six contacts per sphere. Geometrical investigations can be performed on the basis of the corresponding homogeneous sphere packings if all atoms in these structures are replaced by like ones. Then, the respective crystal structures belong to the diamond type or form a primitive cubic lattice. They may be described in supergroups of index 2 of the actual space groups, namely $Fd\bar{3}m$ and $Pm\bar{3}m$, respectively. The former corresponds to the cubic invariant lattice complex *cD* (*International Tables for Crystallography*, 1995*a*, Vol. A, ch. 14) and to a homogeneous sphere packing of type 4/6/*c*1, the latter to the cubic invariant lattice complex *cP* and to a sphere packing of type 6/4/*c*1 (Fischer, 1973).

As in previous work, the assumption was made that no bonds are breaking during the phase transition. In contrast to the transition model described before (Sowa, 2000*b*), threefold axes are maintained during the symmetry reduction. Fig. 1 shows a possible route (in the following, the hexagonal setting is used for all rhombohedral space groups): Starting from a *D* configuration in space group $Fd\bar{3}m$ (origin choice 2), symmetry reduction leads to the translation-equivalent subgroups $R\bar{3}m$ and $R32$. Finally, a class-equivalent subgroup $P3_221$ of $R32$ is obtained. In $P3_221$, the *cD* configuration is found as a limiting form at the general position 6(*c*) with $x = y = \frac{1}{3}$, $z = \frac{1}{8}$ and $c/a = 6^{1/2}$. The symmetry reduction of $Pm\bar{3}m$ leads *via* $R\bar{3}m$ and $R32$ to $P3_121$. To reach the final space group $P3_221$, the *c* lattice parameter must be doubled. The cubic primitive lattice occurs as a limiting form at $x = 0$, $y = \frac{1}{3}$, $z = \frac{1}{12}$ with $c/a = 6^{1/2}$.

The analogous symmetry relations between the zinc-blende and the NaCl type are shown in Fig. 2. Starting from $F4\bar{3}m$, symmetry reduction leads first to $R3m$ and then *via* $R3$ to the final space group $P3_2$. The undistorted zinc-blende type occurs if all atoms are located at Wyckoff position 3(*a*) x,y,z: one kind of atom at $x = y = \frac{1}{3}$, $z = -\frac{1}{8}$ and the other at $x = y = \frac{1}{3}$, $z = \frac{1}{8}$, and if the axial ratio is $c/a = 6^{1/2}$. The ideal NaCl-type arrangement is obtained in $P3_2$ if the atoms occupy the positions at $x = 0$, $y = \frac{1}{3}$, $z = \frac{7}{12}$ and $x = 0$, $y = \frac{1}{3}$, $z = \frac{1}{12}$ and if $c/a = 6^{1/2}$. In this case, the symmetry reduction leads from $Fm\bar{3}m$ *via* $R\bar{3}m$, $R32$ and $R3$ to $P3_2$.

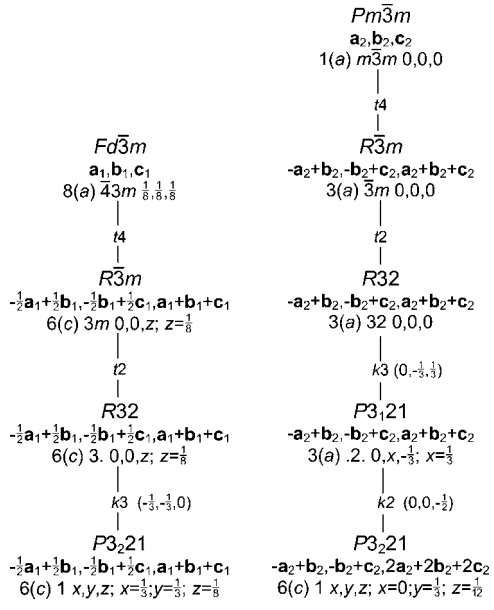

Figure 1
Symmetry relations between a diamond configuration and a cubic primitive lattice.

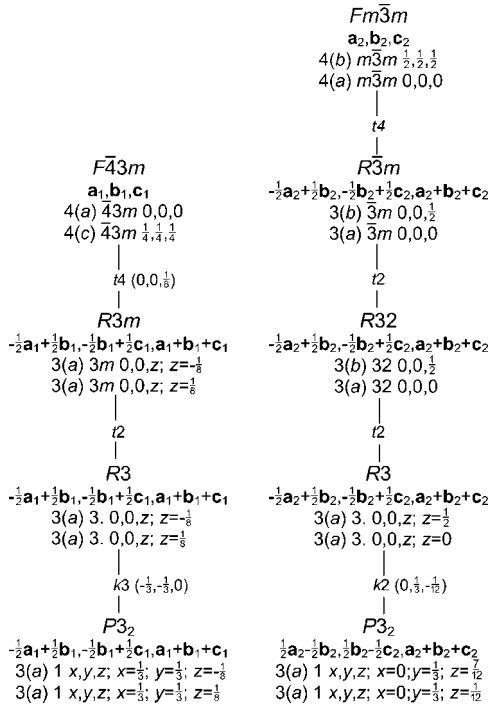

Figure 2
Symmetry relations between the structure types of zinc-blende and NaCl.

Table 1
Symmetry operations that may give rise to sphere contacts to a reference sphere at x,y,z and corresponding coordinates of the generated sphere centres.

A	$y, x, -z$	2	$x, x, 0$
B	$x-y+1, 1-y, \frac{1}{3}-z$	2_1	$(\frac{1}{2}, 0, 0)$ $x, \frac{1}{2}, \frac{1}{6}$
	$x-y, 1-y, \frac{1}{3}-z$	2_1	$(-\frac{1}{2}, 0, 0)$ $x, \frac{1}{2}, \frac{1}{6}$
C	$x-y, -y, \frac{1}{3}-z$	2	$x, 0, \frac{1}{6}$
D	$y, 1+x, -z$	2_1	$(\frac{1}{2}, \frac{1}{2}, 0)$ $x, x+\frac{1}{2}, 0$
	$y-1, x, -z$	2_1	$(-\frac{1}{2}, -\frac{1}{2}, 0)$ $x, x+\frac{1}{2}, 0$
E	$1+x, y, z$	*t*	$(1, 0, 0)$
	$x, y+1, z$	*t*	$(0, 1, 0)$
	$1+x, 1+y, z$	*t*	$(1, 1, 0)$
	$-1+x, y, z$	*t*	$(-1, 0, 0)$
	$x, -1+y, z$	*t*	$(0, -1, 0)$
	$-1+x, -1+y, z$	*t*	$(-1, -1, 0)$
F	$1+y, x, -z$	2_1	$(\frac{1}{2}, \frac{1}{2}, 0)$ $x, x-\frac{1}{2}, 0$
	$y, -1+x, -z$	2_1	$(-\frac{1}{2}, -\frac{1}{2}, 0)$ $x, x-\frac{1}{2}, 0$
G	$1-y, x-y, -\frac{1}{3}+z$	3^+	$(0, 0, -\frac{1}{3})$ $\frac{2}{3}, \frac{1}{3}, z$
	$1+y-x, 1-x, \frac{1}{3}+z$	3^-	$(0, 0, \frac{1}{3})$ $\frac{2}{3}, \frac{1}{3}, z$
H	$1-x, 1-x+y, \frac{2}{3}-z$	2_1	$(0, \frac{1}{2}, 0)$ $\frac{1}{2}, y, \frac{1}{3}$
	$1-x, -x+y, \frac{2}{3}-z$	2_1	$(0, -\frac{1}{2}, 0)$ $\frac{1}{2}, y, \frac{1}{3}$
I	$-x, y-x, \frac{2}{3}-z$	2	$0, y, \frac{1}{3}$
J	$-x, y-x, -\frac{1}{3}-z$	2	$0, y, -\frac{1}{6}$
K	$y, x, 1-z$	2	$x, x, \frac{1}{2}$

3. Description of the *cD* to *cP* phase transition

The structural relations that lead to the transition described above can be studied by examining the possible deformations of sphere packings of type 4/6/*c*1 within the Wyckoff position $P3_221$ 6(*c*) x,y,z. Four parameters may be varied: the three coordinates x,y,z and the axial ratio *c*/*a*. The investigations were performed in the same way as has been described for the transition models derived before (Sowa, 2000*a*,*b*, 2001).

All types of sphere packings with symmetry $P3_221$ 6(*c*) x,y,z were derived, but in the following only those are mentioned that have some relevance for the phase transition under consideration. With the exception of one sphere-packing type with eleven contacts per sphere (*cf. International Tables for Crystallography*, 1995*b*, Vol. C, ch. 9.1) and two types with three contacts (Koch & Fischer, 1995), no information on sphere packings with this symmetry has been available before. All the considerations are of course also valid for the space group $P3_121$ that is enantiomorphic to $P3_221$.

As mentioned before, the diamond configuration corresponds to a sphere packing of type 4/6/*c*1 with four equidistant neighbours per sphere. Referred to a reference sphere with centre at $P3_221$ 6(*c*) x,y,z, the nearest neighbours are located at $y,x,-z$ (*A*); $x-y+1,1-y,\frac{1}{3}-z$ (*B*); $x-y,1-y,\frac{1}{3}-z$ (*B*) and $x-y,-y,\frac{1}{3}-z$ (*C*). Their squared distances from the original sphere are $d_A^2 = (3x^2+3y^2-6xy)a^2+4z^2c^2$, $d_B^2 = (3y^2-3y+1)a^2+(4z^2-\frac{4}{3}z+\frac{1}{9})c^2$ and $d_C^2 = 3y^2a^2+(4z^2-\frac{4}{3}z+\frac{1}{9})c^2$, respectively. The sphere-packing conditions for 4/6/*c*1 in $P3_221$ 6(*c*) are obtained by equating these distances:

$$y = \tfrac{1}{3} \quad \text{and} \quad (3x^2 - 2x)a^2 + (\tfrac{4}{3}z - \tfrac{1}{9})c^2 = 0. \qquad (1)$$

Within the general position of $P3_221$, the type 4/6/*c*1 has two degrees of freedom. Its parameter region is bounded by that of 12 sphere-packing types with one or no degree of freedom (*cf.* Fig. 3). Provided that the reference sphere at x,y,z lies within the described parameter region of 4/6/*c*1 or at its boundary, altogether 21 symmetry operations may give rise to a contact with a neighbouring sphere. For symmetry reasons, two or more neighbouring spheres may be equidistant from the original sphere. Therefore, only 11 different kinds of possible neighbours have to be distinguished, which are labelled *A* to *K* (*cf.* Table 1). The occurring sphere-packing types are listed in Table 2. For each type, the highest possible symmetry is given together with some simple parameter conditions that must be fulfilled in addition to (1). The parameter regions of six types of sphere packings with one degree of freedom (generation class 1.1 to 1.6) and five types with no degree of freedom (0.1 to 0.5′) surround the parameter region of 4/6/*c*1 (2.1). Sphere packings of type 8/4/*c*1 occur twice (0.5 and 0.5′). They are equivalent with respect to a twofold rotation of the Euclidean normalizer $N_E(P3_221) = P6_422$ with $\mathbf{a}' = \mathbf{a}+\mathbf{b}$, $\mathbf{b}' = -\mathbf{a}$, $\mathbf{c}' = \frac{1}{2}\mathbf{c}$ (*International Tables for Crystallography*, 1995*a*, Vol. A, ch.

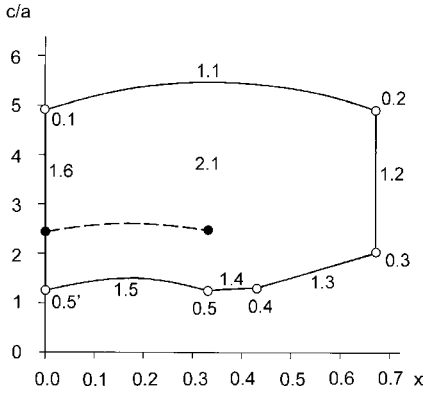

Figure 3
The parameter regions of sphere-packing types bounding 4/6/*c*1 in $P3_221$ 6(*c*) x,y,z with $0 \le x \le \frac{2}{3}$, $y = \frac{1}{3}$ and $\frac{1}{12} \le z \le \frac{1}{4}$. All sphere packings are designated by the corresponding generation classes *g.h* [*g*: number of degrees of freedom, *h*: arbitrary number (*c.f.* Fischer, 1991)]. The solid circles show the parameters of an ideal diamond arrangement (2.1) and of a cubic primitive lattice (1.6). The dashed line marks the proposed transition path.

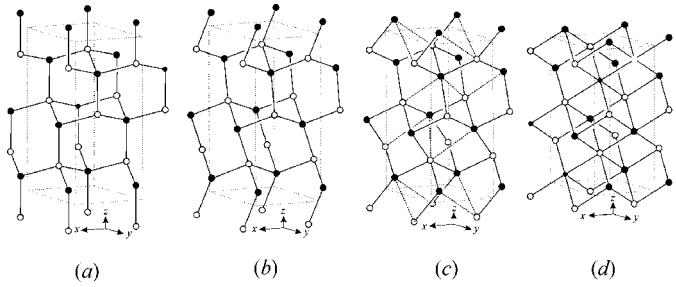

Figure 4
Schematic representation of the structural variations during the transformation from the zinc-blende to the NaCl type along the proposed transition path. Open and solid circles correspond to the different kinds of atoms. (*a*) Ideal zinc-blende type, atoms at 3(*a*) x,y,z, with $x = y = \frac{1}{3}$, $z = \frac{1}{8}$ and with $x = y = \frac{1}{3}$, $z = -\frac{1}{8}$, $c/a = 6^{1/2}$. Different *AB* double layers are linked by bonds parallel to the *c* axis. (*b*) Intermediate structure with atomic coordinates: $x = 0.2$, $y = \frac{1}{3}$, $z = 0.115$ and $x = \frac{1}{3}$, $y = 0.2$, $z = -0.115$, $c/a = 2.592$. (*c*) Intermediate structure with atomic coordinates: $x = 0.1$, $y = \frac{1}{3}$, $z = 0.103$ and $x = \frac{1}{3}$, $y = 0.1$, $z = -0.103$, $c/a = 2.575$. Dashed lines show the additional neighbours in the NaCl type. (*d*) Ideal NaCl type, atomic coordinates: $x = 0$, $y = \frac{1}{3}$, $z = \frac{1}{12}$ and $x = \frac{1}{3}$, $y = 0$, $z = -\frac{1}{12}$, $c/a = 6^{1/2}$.

Table 2
Sphere-packing types adjacent to 4/6/*c*1 in $P3_221$ 6(*c*).

Sphere packings are symbolized with *k*/*m*/*fn* according to a proposal by Fischer (1973): *k* is the number of contacts per sphere, *m* is the size of the shortest mesh, *f* indicates the highest crystal family for packings of that type, *n* is an arbitrary number.

Generation class	Neighbouring points	Additional conditions		Sphere-packing type	Highest symmetry
2.1	*ABC*			4/6/*c*1	$Fd\bar{3}m$ 8(*a*)
1.1	*ABCE*			10/3/*h*4	$R\bar{3}m$ 6(*c*)
1.2	*ABCF*	$x = \frac{2}{3}$, $z = \frac{1}{12}$		6/4/*h*2	$P6_3/mmm$ 2(*c*)
1.3	*ABCG*			6/3/*h*11	$P3_221$ 6(*c*)
1.4	*ABCH*			6/4/*h*4	$P3_221$ 6(*c*)
1.5	*ABCI*			5/4/*h*11	$P6_222$ 6(*i*)
1.6	*ABCD*	$x = 0$, $z = \frac{1}{12}$		6/4/*c*1	$Pm\bar{3}m$ 1(*a*)
0.1	*ABCDE*	$x = 0$, $z = \frac{1}{12}$, $c/a = 2\times6^{1/2}$	$\rho = 74.0\%$	12/3/*c*1	$Fm\bar{3}m$ 4(*a*)
0.2	*ABCEF*	$x = \frac{2}{3}$, $z = \frac{1}{12}$, $c/a = 2\times6^{1/2}$	$\rho = 74.0\%$	12/3/*h*1	$P6_3/mmm$ 2(*c*)
0.3	*ABCFG*	$x = \frac{2}{3}$, $z = \frac{1}{12}$, $c/a = 2$	$\rho = 53.7\%$	8/3/*h*3	$P6_3/mmm$ 2(*c*)
0.4	*ABCGH*	$x = 0.4322$, $z = 0.2190$, $c/a = 1.29654$	$\rho = 58.4\%$	8/3/*h*5	$P3_221$ 6(*c*)
0.5	*ABCHIK*	$x = \frac{1}{3}$, $z = \frac{1}{4}$, $c/a = \frac{1}{2}6^{1/2}$,	$\rho = 68.0\%$	8/4/*c*1	$Im\bar{3}m$ 2(*a*)
0.5′	*ABCDIJ*	$x = 0$, $z = \frac{1}{12}$, $c/a = \frac{1}{2}6^{1/2}$	$\rho = 68.0\%$	8/4/*c*1	$Im\bar{3}m$ 2(*a*)

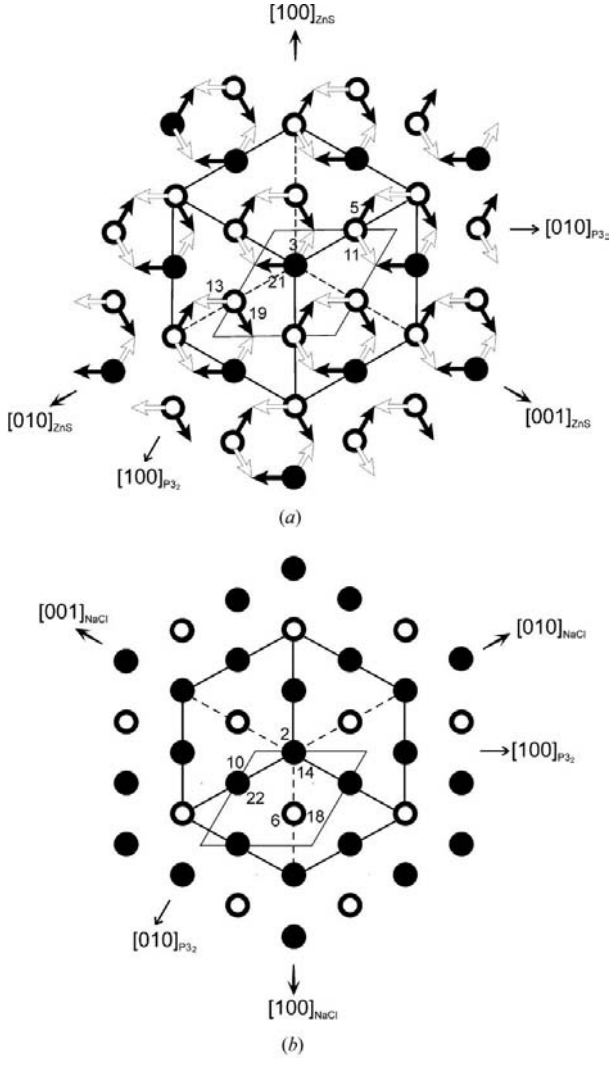

Figure 5
Schematic representation of the proposed transition mechanism from the zinc-blende to the NaCl type. The unit cell of $P3_221$ is outlined. White and black circles indicate the two types of atom. The *z* coordinates of the atoms are given in *n*/24. (*a*) Atomic arrangement of a zinc-blende-type structure. One unit cell is shown projected along [111]. Arrows indicate the atomic shifts. (*b*) NaCl-type structure after the phase transition.

15). In Fig. 3, the parameter region of 4/6/*c*1 and its boundaries are projected on the *x*–*c*/*a* plane.

The ideal diamond configuration *cD* is realized in $P3_221$ at $\frac{1}{3},\frac{1}{3},\frac{1}{8}$ with $c/a = 6^{1/2}$. Sphere packings of type 6/4/*c*1 occur with one degree of freedom (1.6 in Fig. 3). The undistorted *cP* configuration is found at $0,\frac{1}{3},\frac{1}{12}$ with $c/a = 6^{1/2}$. During the deformation, all atoms move by $\frac{1}{3}$ of the *a* lattice parameter and $\frac{1}{24}$ of the *c* lattice parameter within planes that are parallel to {100}. In order to describe the transformation process graphically, it is advantageous to regard double layers of spheres perpendicular to **c** (*c.f.* Fig. 4). Then, the transformation is characterized by the shift of such double layers along the ⟨100⟩ directions by $\frac{1}{3}a$ while simultaneously the distances within one double layer increase because the two single layers are shifted in opposite directions by $\frac{1}{24}c$.

Fig. 5 shows the corresponding changes during the transformation from the zinc-blende to the NaCl type. If, for example, an *A* layer together with its neighbouring *B* layer is shifted along [110], the double layers below and above move along $[\bar{1}00]$ and $[0\bar{1}0]$, respectively. At the same time, the *a* lattice parameter shrinks. As a consequence, one of the ⟨111⟩ directions of the structure with zinc-blende type runs parallel to one of the ⟨111⟩ directions of the NaCl-type structure. The NaCl-type unit cell is rotated by 180° around this direction compared with that of the zinc-blende type.

As noted in previous papers (Sowa, 2000*a*,*b*, 2001), in principle, each route through the two-dimensional parameter field of 4/6/*c*1 is a possible transition path and the true path cannot be determined geometrically. Therefore, similar to the transformation described by Sowa (2000*b*), a second model for the zinc-blende to NaCl-type transition is proposed here that maintains the four nearest neighbours and, in addition, 10 of the next-nearest neighbours equidistant from the reference atom.

The additional condition for such a one-dimensional transition pathway is:

$$x = \tfrac{1}{6} \pm \tfrac{1}{3}[\tfrac{9}{4} - \tfrac{1}{3}(c^2/a^2)]^{1/2}. \qquad (2)$$

The corresponding path is marked in Fig. 3.

Fig. 6 shows the variations of the unit-cell parameters for such a model during the transformation calculated with normalized interatomic distances. Fig. 7(*a*) displays the corresponding normalized interatomic distances. For comparison, the analogous distances for the transition model with orthorhombic symmetry (Sowa, 2000*b*) are shown in Fig. 7(*b*). The two figures are very similar. Distinct differences do not occur until the third coordination shell of the NaCl type. Therefore, it may be supposed that the two transition mechanisms are very similar from an energetic point of view. Since in the present model close-packed atomic planes are maintained during the whole transformation (*c.f.* Fig. 4), such a transition mechanism is possibly preferred.

Until now, there has been no experimental evidence that one of these mechanisms occurs in *AB* compounds. Also, no compound is known showing the structure of one of the intermediate phases. Instead, intermediate high-pressure phases of HgTe (San-Miguel *et al.*, 1995), CdTe (McMahon *et al.*, 1993; Nelmes *et al.*, 1993; Martínez-García *et al.*, 1999), ZnTe (Nelmes *et al.*, 1995) and GaAs (McMahon & Nelmes, 1997) were detected crystallizing with the so-called cinnabar structure type. In theoretical investigations, cinnabar-type phases of CdTe (Ahuja *et al.*, 1997) and GaAs (Mujica *et al.*, 1999) were also found to be stable or metastable, respectively. Côté *et al.* (1997) predicted the existence of such a phase for ZnSe also.

4. Comparison with the cinnabar type

Cinnabar HgS itself crystallizes with space group $P3_221$ or with the enantiomorphic group $P3_121$. In $P3_121$, the Hg atoms occupy positions 3(*a*) $x,0,\frac{1}{3}$ with $x = 0.720$, the S atoms are located at 3(*b*) $x,0,\frac{5}{6}$ with $x = 0.485$. The axial ratio is $c/a = 2.291$ (Aurivillius, 1950). Each atom is twofold coordinated so that helical chains parallel to the *c* axis are formed. Such a structure has also been observed for HgO (Aurivillius & Carlsson, 1958). The structure type of the intermediate high-pressure phases of HgSe, HgTe and CdTe that occur between the zinc-blende and the NaCl type is called cinnabar type because it has the same space group as cinnabar and the same Wyckoff positions are occupied. However, the positional parameters of the atoms and, consequently, their coordinations are quite different. The approximate coordinates are 3(*a*) $x,0,\frac{1}{3}$ with $x \simeq 0.64$ and 3(*b*) $x,0,\frac{5}{6}$ with $x \simeq 0.56$. The axial

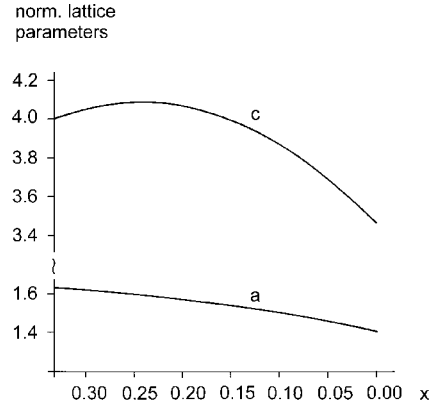

Figure 6
Variations of the normalized lattice parameters (shortest interatomic distance $d = 1$) depending on the positional parameter x during the transformation from the zinc-blende to the NaCl type (model with ten equal distances to the next-nearest neighbours during the transition).

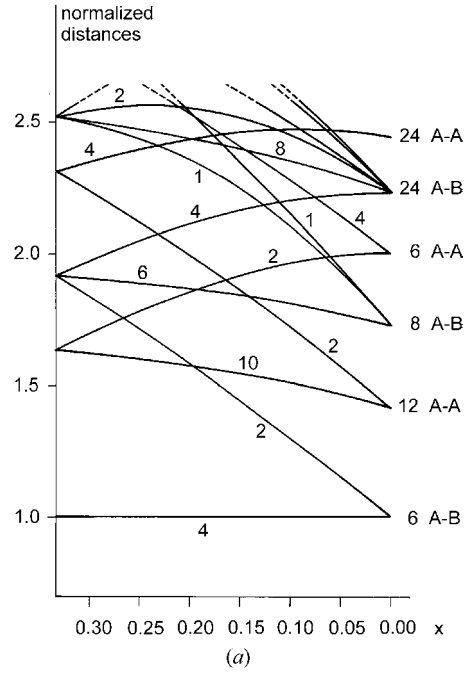

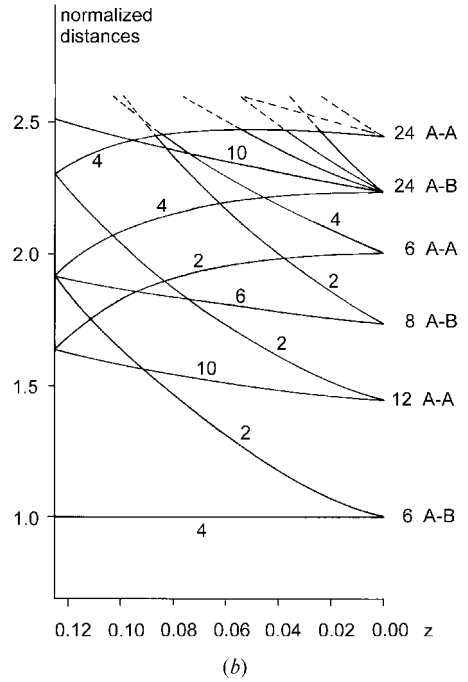

Figure 7
(*a*) Variations of the normalized interatomic distances (shortest interatomic distance $d = 1$) depending on the positional parameter x during the transformation from the zinc-blende to the NaCl type according to the proposed transition model in $P3_2$. (*b*) Variations of the corresponding distances according to the transition model in *Imm*2 (Sowa, 2000*b*). *A*–*A* and *A*–*B* denote distances between like and unlike atoms, respectively. The numbers of equal distances are given.

ratios vary between $c/a \simeq 2.28$ and $c/a \simeq 2.39$. Each atom is surrounded by four neighbours of the other kind forming a distorted tetrahedron. In GaAs and ZnTe, the so-called cinnabar type occurs as an intermediate high-pressure phase between the zinc-blende and the *Cmcm* type. The axial ratios are $c/a \simeq 2.23$ and $c/a \simeq 2.29$, respectively. The free parameters of the atoms are $x \simeq 0.54$ and $x \simeq 0.50$ in both structures. All atoms are also fourfold coordinated, but the distances from the next-nearest neighbours are considerably longer than in HgSe, HgTe and CdTe.

The maximal expanded structure of the cinnabar type occurs in $P3_221$ if the atoms are located at Wyckoff positions $3(a)$ $x,0,\frac{2}{3}$ with $x = \frac{1}{2}$ and $3(b)$ $x,0,\frac{1}{6}$ with $x = \frac{1}{2}$ and the axial ratio is $c/a = \frac{3}{2}2^{1/2} \simeq 2.1213$. It corresponds to a heterogeneous sphere packing with four contacts. Such a configuration can be deformed without losing contacts into a sixfold coordinated NaCl-type arrangement with atoms at $3(a)$ $x,0,\frac{2}{3}$, with $x = \frac{1}{3}$ and $3(b)$ $x,0,\frac{1}{6}$ with $x = \frac{1}{3}$ and $c/a = 6^{1/2}$. Thus, starting from the NaCl type, the cinnabar type as well as the proposed type with symmetry $P3_2$ could be obtained under decreasing pressure. Figs. 8(*a*) and 8(*b*) show the pattern of bonds that must be broken for these transformations. The broken bonds form zigzag chains parallel to three of the ⟨110⟩ directions if the $P3_2$ type occurs and they are arranged in screws parallel to one of the ⟨111⟩ directions if the transition leads to the cinnabar type.

In the two types, the linkage between the atoms differs. The $P3_2$ type can be deformed until the zinc-blende type is reached, whereas such a displacive transition is not possible when coming from the cinnabar type. In the latter case, at least two bonds per atom have to be broken and two new neighbours must enter the coordination sphere of each atom to obtain the zinc-blende type.

The question arises whether one of the theoretically derived intermediate phases may exist at high pressure. As mentioned above, the existence of the $P3_2$ type seems to be more probable than that of the *Imm*2 type. Unfortunately, the X-ray powder pattern of the hypothetical $P3_2$ type would be very similar to that of the cinnabar type. The ideal structure described above is not very likely for real compounds, since atoms may not act as hard spheres but are covalently bonded to the adjoining ones. If one allows small deviations of the ideal transition path, the axial ratio that is $c/a > 6^{1/2}$ along the ideal transformation path may become slightly less than $6^{1/2} \simeq 2.45$ and thus the lattice parameters may have the same values as those measured for the intermediate phases of the cinnabar type. If, in addition, slight distortions of the coordination polyhedra occur leading to interatomic distances comparable with those reported for the cinnabar type, the powder diagrams of the two types may become very similar. Therefore, it will be difficult to identify unambiguously the structure of the intermediate phase from a powder pattern, especially if it is affected by preferred orientation. Fig. 9 displays the simulated powder pattern of the intermediate cinnabar-type phase of CdTe at 3.48 GPa (data from McMahon *et al.*, 1993) in comparison to that of a slightly distorted hypothetical $P3_2$-type phase of CdTe.

Kusaba & Weidner (1994) described the structure of the intermediate phase of ZnTe in space group $P3_1$. The structural parameters are between those for the present transition model described above and those in the cinnabar type.

Energetical calculations are strongly required for finding out whether the proposed intermediate phases may be realized in some compounds as stable or metastable phases,

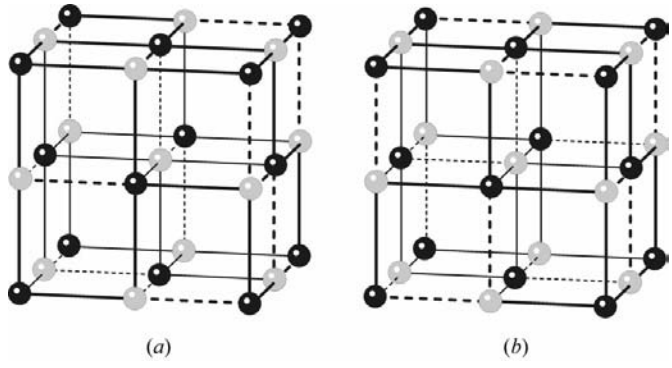

Figure 8
Pattern of breaking bonds for the phase transition from the NaCl to (*a*) the zinc-blende and (*b*) the cinnabar type.

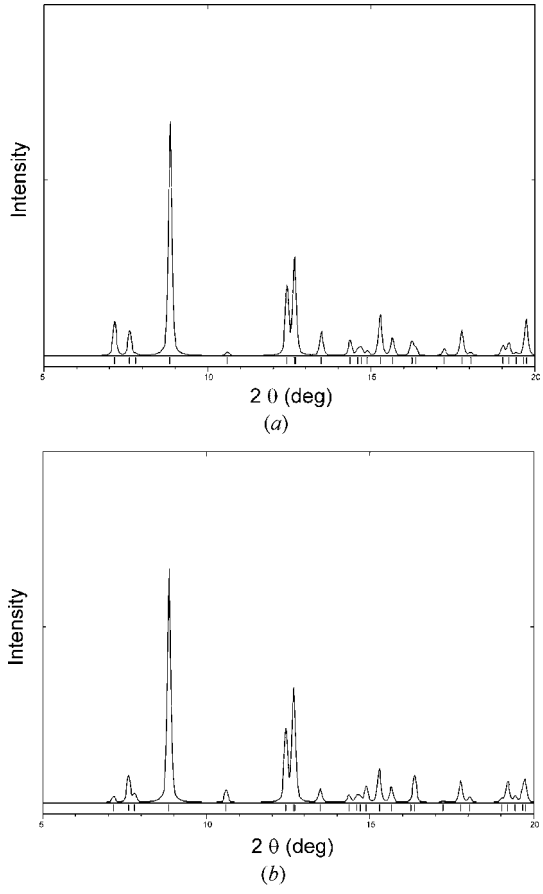

Figure 9
Simulated powder pattern (λ = 0.4650 Å) of (*a*) cinnabar-type CdTe at 3.48 GPa with $a = 4.301$, $c = 10.225$ Å. Cd at $3(a)$ $x,0,\frac{1}{3}$, with $x = 0.631$, Te at $3(b)$ $x,0,\frac{5}{6}$, with $x = 0.568$ (data from McMahon *et al.*, 1993) and (*b*) hypothetical $P3_2$-type CdTe with the same lattice parameters and Cd at $3(a)$ x,y,z, with $x = 0.075$, $y = \frac{1}{3}$, $z = 0.07$ and Te at $3(a)$ x,y,z with $x = \frac{1}{3}$, $y = 0.075$, $z = -0.07$.

whether they may only occur during the direct transformation from the zinc-blende to the NaCl type, or whether they are not favourable at all compared with other phases.

I would like to thank Professor Elke Koch, Marburg, for many helpful discussions and critical reading of the manuscript.

References

Ahuja, R., James, P., Eriksson, O., Wills, J. M. & Johansson, B. (1997). *Phys. Status Solidi B*, **199**, 75–79.
Aurivillius, K. L. (1950). *Acta Chem. Scand.* **4**, 1413–1436.
Aurivillius, K. & Carlsson, I. B. (1958). *Acta Chem. Scand.* **12**, 1297–1304.
Catti, M. (2001). *Phys. Rev. Lett.* **87**, 35504.
Christy, A. G. (1993). *Acta Cryst.* B**49**, 987–996.
Côté, M., Zakharov, O., Rubio, A. & Cohen, M. L. (1997). *Phys. Rev. B*, **55**, 13025–13031.
Dmitriev, V. P., Rochal, S. B., Gufan, Yu. M. & Toledano, P. (1988). *Phys. Rev. Lett.* **60**, 1958–1961.
Fischer, W. (1973). *Z. Kristallogr.* **138**, 129–146.
Fischer, W. (1991). *Z. Kristallogr.* **194**, 67–85.
Froyen, S. & Cohen, M. L. (1983). *Phys. Rev. B*, **28**, 3258–3265.
International Tables for Crystallography (1995*a*). Vol. A, edited by Th. Hahn. Dordrecht: Kluwer Academic Publishers.
International Tables for Crystallography (1995*b*). Vol. C, edited by A. J. C. Wilson. Dordrecht: Kluwer Academic Publishers.
Koch, E. & Fischer, W. (1995). *Z. Kristallogr.* **210**, 407–414.
Kusaba, K. & Weidner, D. J. (1994). *Proc. AIRAPT/APT Meeting 1993, High-Pressure Science and Technology*, edited by S. C. Schmidt, J. W. Shaner, G. A. Samara & M. Ross, pp. 553–556. New York: American Institute of Physics.
McMahon, M. I. & Nelmes, R. J. (1997). *Phys. Rev. Lett.* **78**, 3697–3700.
McMahon, M. I., Nelmes, R. J., Wright, N. G. & Allan, D. R. (1993). *Phys. Rev. B*, **48**, 16246–16251.
Martínez-García, D., Le Godec, Y., Mézouar, M., Syfosse, G., Itié, J. P. & Besson, J. M. (1999). *Phys. Status Solidi B*, **211**, 461–467.
Mujica, A., Muñoz, A., Radescu, S. & Needs, R. J. (1999). *Phys. Status Solidi B*, **211**, 345–350.
Nelmes, R. J., McMahon, M. I., Wright, N. G. & Allan, D. R. (1993). *Phys. Rev. B*, **48**, 1314–1317.
Nelmes R. J., McMahon M. I., Wright, N. G. & Allan, D. R. (1995). *J. Phys. Chem. Solids*, **56**, 545–549.
O'Keeffe, M. & Hyde, B. G. (1996). *Crystal Structures. I. Patterns and Symmetry*. Washington: Mineralogical Society of America.
San-Miguel, A., Wright, N. G., McMahon, M. I. & Nelmes, R. J. (1995). *Phys. Rev. B*, **51**, 8731–8736.
Shimojo, F., Ebbsjö, I., Kalia, R. K., Nakano, A., Rino, J. P. & Vashishta, P. (2000). *Phys. Rev. Lett.* **84**, 3338–3341.
Sowa, H. (2000*a*). *Acta Cryst.* A**56**, 288–299.
Sowa, H. (2000*b*). *Z. Kristallogr.* **215**, 335–342.
Sowa, H. (2001). *Acta Cryst.* A**57**, 176–182.
Ves, S., Schwarz, U., Christensen, N. E., Syassen, K. & Cardona, M. (1990). *Phys. Rev. B*, **42**, 9113–9118.
Wentzcovitch, R. M., Cohen, M. L. & Lam, P. K. (1987). *Phys. Rev. B*, **36**, 6058–6068.
Zunger, A., Kim, K. & Ozolins, V. (2001). *Phys. Status Solidi B*, **223**, 369–378.